

ENHANCED STRESS PREDICTION CORRELATION FOR ABDOMINAL
AORTIC ANEURYSM USING FLUID STRUCTURE INTERACTION
TECHNIQUE

BADREDDIN GIUMA S.K ELGHARIANI

A thesis submitted in fulfilment of the
requirements for the award of the degree of
Doctor of Philosophy (Mechanical Engineering)

Faculty of Mechanical Engineering
Universiti Teknologi Malaysia

AUGUST 2013

ACKNOWLEDGEMENT

I would like to express my sincere appreciation to my thesis supervisors Assoc.Prof.Dr Kahar Osman and Assoc.Prof.Ir.Dr Mohamed Refiq Abdul Kadir for their continuous interest support and guidance during my studies without their advices and motivation, this thesis would not have been the same as presented.

I am indebted to my colleagues in the groups of MediTeq, and CFM, as well as all my friends who have provided assistance and advice at various occasion.

I would also like to thank Malaysian Ministry of Higher Education (MOHE) and Universiti Teknologi Malaysia (UTM) for providing research grant during the first of the two years of my study.

My deepest gratitude goes to my whole family, especially to my father and mother for their love encourage and support through the years.

ABSTRACT

The rupture of the abdominal aortic aneurysm (AAA) occurs when the acting stress exceeds the ultimate stress of the wall. Therefore, the ability to accurately estimate the acting stress is very useful to predict the rupture of an AAA. In this study, previously developed equation which included the effect of inter lumen thrombus, systolic pressure, maximum aneurysm diameter, wall thickness, asymmetry parameter, is improved by applying fully coupling-fluid structure interaction technique (f-FSI). Further improvements of the equation is also done by including the aneurysm length and iliac bifurcation angle. Various case studies are analyzed to investigate the hemodynamic behavior as well as stress distribution on the wall using modified models as well as Computed Tomography scan (CT scan). The results show that the geometry parameters as well as hypertension affect the flow pattern, displacement and stress distribution. Exponential correlation is observed between the maximum acting stress and the asymmetric parameter. In addition, a linear correlation with the maximum aneurysm, aneurysm length, iliac bifurcation angle and wall thickness is determined. The parametric correlations confirm that these geometry parameters are important parameters to predict the maximum acting stress. The inclusion of the effect of hemodynamic by using f-FSI technique predicted a higher maximum acting stress in AAA wall compared to previous equations. Consequently, the current research has concluded that the newly developed equation can be easily used for rupture prediction with even more accurate results than the currently used clinical tools.

ABSTRAK

Aneurisme aortik abdomen (AAA) akan pecah apabila tegasan yang bertindak melebihi tegasan muktamad dinding. Oleh itu, kebolehan untuk meramal secara tepat tekanan yang bertindak sangat berguna untuk meramal bila dinding AAA akan pecah. Dalam kajian ini, persamaan yang telah dibangunkan terdahulu yang merangkumi kesan daripada "lumen thrombus" dalaman, tekanan "systolic", diameter maksimum aneurisme, ketebalan dinding, kesan tidak simetri, diperbaiki dengan mengaplikasikan teknik gandigan penuh interaksi antara cecair dan struktur (f-FSI). Penambahbaikan persamaan juga dilakukan dengan mengambil kira panjang aneurisme dan sudut pencabangan dua iliak. Pelbagai kajian kes dianalisis untuk mengenal pasti tingkah laku hemodinamik serta taburan tekanan pada dinding dengan menggunakan model yang telah diubahsuai serta imbasan Tomografi Berkomputer (CT scan). Keputusan menunjukkan bahawa geometri serta tekanan darah tinggi memberi kesan kepada corak aliran, anjakan dan taburan tekanan. Terdapat korelasi eksponen antara tekanan maksimum yang bertindak dan parameter tidak simetri. Di samping itu, hubungan linear dengan aneurisma maksimum, panjang aneurisme, sudut pencabangan dua iliak dan ketebalan dinding ditentukan. Perkaitan parametrik mengesahkan parameter geometri adalah parameter penting untuk meramalkan tekanan bertindak maksimum. Penggunaan kesan hemodinamik dengan menggunakan teknik f-FSI meramalkan tekanan maksimum yang lebih tinggi bertindak pada dinding AAA berbanding dengan persamaan sebelumnya. Di akhir penyelidikan ini, dapat disimpulkan bahawa persamaan baru yang dibangunkan ini boleh digunakan dengan mudah untuk meramal pecah dengan hasil yang lebih tepat dibandingkan dengan alatan klinikal sedia ada.

TABLE OF CONTENTS

| CHAPTER | TITLE | PAGE |
|-----------|--|-----------|
| | DECLARATION | ii |
| | DEDICATION | iii |
| | ACKNOWLEDGEMENTS | iv |
| | ABSTRACT | v |
| | ABSTRAK | vi |
| | TABLE OF CONTENTS | vii |
| | LIST OF TABLES | ix |
| | LIST OF FIGURES | x |
| | LIST OF SYMBOLS | xiv |
| | LIST OF APPENDICES | xviii |
| 1. | INTRODUCTION | 1 |
| | 1.1 Introduction | 1 |
| | 1.2 problem Statement | 4 |
| | 1.3 Objectives of the study | 5 |
| | 1.4 Scopes of the study | 5 |
| | 1.5 Outline of thesis | 6 |
| 2. | LITERATURE REVIEW | 8 |
| | 2.1 Introduction | 8 |
| | 2.2 Literature review | 8 |
| 3. | METHODOLOGY | 17 |
| | 3.1 Introduction | 17 |
| | 3.2 Identify the physiological variables | 19 |

| | | |
|-----------|---|------------|
| 3.3 | Three dimensional real geometry reconstruction | 24 |
| 3.4 | Formulation of fluid structure interaction | 25 |
| 3.4.1 | Governing equations for fluid domain | 26 |
| 3.4.2 | Governing equations for solid domain | 29 |
| 3.4.3 | Boundary conditions | 31 |
| 3.4.4 | Numerical procedure | 36 |
| 3.5 | The new equation to predict the maximum acting stress in AAA wall | 53 |
| 4. | RESULTS AND DISCUSSION | 59 |
| 4.1 | Introduction | 59 |
| 4.2 | Validation | 60 |
| 4.3 | The effect Newtonian and Non-Newtonian properties on the wall shear stress distribution, and flow phenomena | 63 |
| 4.4 | The effect of the maximum aneurysm diameter on the flow pattern, the displacement and stress distribution | 70 |
| 4.5 | The effect of the aneurysm length on the flow pattern, the displacement and stress distribution | 78 |
| 4.6 | The effect of the length of the distal neck on the flow pattern, the displacement and stress distribution | 83 |
| 4.7 | The effect of the iliac bifurcation angle on the flow pattern, the displacement and stress distribution | 88 |
| 4.8 | The effect of the asymmetry on the flow pattern, the displacement and stress distribution | 93 |
| 4.9 | The effect of the wall thickness on the flow pattern, the displacement and stress distribution | 98 |
| 4.10 | The effect of the hypertension on the flow pattern, the displacement and stress distribution | 102 |
| 4.11 | The new model to predict the maximum acting stress in the AAA | 112 |
| 5. | CONCLUSION | 117 |
| 5.1 | Conclusion | 117 |
| 5.2 | Limitations and Recommendations | 119 |
| | REFERENCES | 122 |
| | Appendix-A | 133 |

LIST OF TABLES

| TABLE NO. | TITLE | PAGE |
|------------------|--|-------------|
| 3.1 | Comparison of Newtonian and various Non-Newtonian models for blood | 28 |
| 3.2 | The interpolation functions for the velocity component parallel, and perpendicular to the three side of the element | 42 |
| 4.1 | The maximum displacement magnitude in the solid analysis, and the maximum velocity magnitude in the fluid analysis for three different mesh size | 61 |
| 4.2 | The comparison between our result and Scotti et al [54] at model ($L_{an}=12$ cm, $D_{an}=6$ cm, and $\beta=1$) | 62 |
| 4.3 | Comparisons between the three models and published data sets | 115 |
| 4.4 | Comparisons between the three models and FSI analysis of the real AAA driving form CT Scan | 116 |
| 4.5 | Comparisons between the three models and FSI analysis of modified models of AAA | 116 |

LIST OF FIGURES

| FIGURES NO. | TITLE | PAGE |
|-------------|--|------|
| 1.1 | Fluid-Structure Interaction analyses producer | 3 |
| 3.1 | The flow chart for the procedure to developed the new equation to predict the maximum acting stress in AAA | 18 |
| 3.2 | Parameter measurements of abdominal aortic aneurysm | 23 |
| 3.3 | 3D geometry reconstruction | 25 |
| 3.4 | Schematics of AAA with the boundary conditions for fluid domain | 32 |
| 3.5 | Transient behavior of the boundary conditions | 33 |
| 3.6 | Schematics of AAA with the boundary conditions for solid domain | 34 |
| 3.7 | Tetrahedral element for the fluid domain and solid domain | 36 |
| 3.8 | The interpolation of velocity at fluid nodal using solid nodal | 41 |
| 3.9 | The interpolation of velocity at fluid nodal using fluid nodal | 46 |
| 3.10 | Solution process for direct method | 52 |
| 4.1 | Time periodic convergence for the velocity magnitude and displacement magnitude at five difference nod | 62 |
| 4.2 | Comparison of velocity vectors between Newtonian and Non-Newtonian cases through an aneurysm ($D_{an}=6, \beta=1$) at different stages of the second cardiac cycle | 64 |
| 4.3 | Velocity difference along the centre line of an aneurysm between Newtonian and the Carreau model (A) and the Newtonian, and the Carreau Yasuda model (B) within various aneurysm diameters ($D_{an}=3, 4, 5, \text{ and } 6$), at 1.2s | 66 |

| | | |
|------|---|----|
| 4.4 | Comparison of velocity vectors between Newtonian and Non-Newtonian cases through an aneurysm ($D_{an}=6$, $t=1.2$) at different asymmetry parameters $\beta=1,4$, and 7 | 66 |
| 4.5 | Comparison of pressure along the centre line of an aneurysm ($D_{an}=6, \beta=1$) between Newtonian and Non-Newtonian cases at different stages of the second cardiac cycle | 68 |
| 4.6 | Pressure different along the centre line of an aneurysm between the Newtonian and Carreau model, and the Newtonian and the Carreau Yausda model within various aneurysm diameters ($D_{an}=3, 4,5, 6$ cm), at 1.2s | 69 |
| 4.7 | WSS Difference along the aneurysm wall between Newtonian and the Carreau model (A) and the Newtonian and Carreau Yausda model at $t=1.4s$ within various aneurysm diameters($D_{an}=3,4,5,6cm$) | 69 |
| 4.8 | WSS Difference along the aneurysm wall between Newtonian and the Carreau model (A) and the Newtonian and Carreau Yausda model at $t=1.4s$ for different symmetries ($\beta=1, 4$, and 7) | 70 |
| 4.9 | The velocity vectors at different stage of the second cardiac cycle through a deferent aneurysm diameter (3,4,9,10cm) | 72 |
| 4.10 | The distributions of the Displacement Magnitude at different periods of the second cardiac cycle in model ($D_{an}=6, \beta=1$) | 73 |
| 4.11 | The distributions of the Von Mises stress at different periods of the second cardiac cycle in model ($D_{an}=6, \beta=1$) | 74 |
| 4.12 | The distributions of the Displacement Magnitude on the inner(left) and outer (right) wall at peak systolic pressure condition (1.4 s) | 75 |
| 4.13 | The distributions of the Von Mises stress on the inner (left) and outer (right) wall at peak systolic pressure condition (1.4 s) | 75 |
| 4.14 | The Von Mises Stress along the line on the inner wall (line), and the outer wall (dash line) with different maximum diameter at peak systolic pressure condition | 77 |
| 4.15 | Comparison between the Laplace Equation, Z.LI Equation, the FSI solution and the linear fitting of the FSI solution with different maximum diameter | 78 |
| 4.16 | The velocity vectors at different stage of the second cardiac cycle through an aneurysm ($D_{an}=5, L_{an}=9$), ($D_{an}=5, L_{an}=12$), and ($D_{an}=5, L_{an}=15$), | 81 |

| | | |
|------|---|----|
| 4.17 | The distributions of the Displacement Magnitude with different length of aneurysm at peak systolic pressure condition | 82 |
| 4.18 | The distributions of the Von Mises stress with different length of aneurysm at peak systolic pressure condition | 82 |
| 4.19 | Comparison between the Laplace Equation, Z.LI Equation the FSI solution and the linear fitting of the FSI solution with different aneurysm length | 83 |
| 4.20 | The velocity vectors at different stage of the second cardiac cycle through an aneurysm ($D_{an}=6$ cm, $L_{an}=12$ cm, $L_2=0.8$), and ($D_{an}=6$, $L_{an}=12$, $L_2=5$ cm) | 86 |
| 4.21 | The distributions of the Displacement Magnitude with different length distal neck at peak systolic pressure condition | 87 |
| 4.22 | The distributions of the Von Mises stress with different length distal neck at peak systolic pressure condition | 87 |
| 4.23 | The maximum the Von Mises stress as function of the length distal neck | 88 |
| 4.24 | The velocity vectors at different stage of the second cardiac cycle through the two models at different iliac bifurcation angle ($\phi_i = 50^\circ$, and 90°) | 90 |
| 4.25 | The distributions of the Displacement Magnitude with different iliac bifurcation angle at peak systolic pressure condition | 91 |
| 4.26 | The distributions of the Von Mises stress with different iliac bifurcation angle at peak systolic pressure condition | 91 |
| 4.27 | Comparison between the Laplace Equation, Z.LI Equation the FSI solution and the linear fitting of the FSI solution with different iliac bifurcation angle | 92 |
| 4.28 | The velocity vectors at different stage of the second cardiac cycle through the three models at different asymmetry parameter ($\beta = 1, 1/3, \text{ and } 1/5$) | 95 |
| 4.29 | The distributions of the Displacement Magnitude with different asymmetry parameter at peak systolic pressure condition | 96 |
| 4.30 | The distributions of the Von Mises stress with different asymmetry parameter at peak systolic pressure condition | 96 |
| 4.31 | The Von Mises Stress along the line on the anterior inner wall the anterior outer wall, the posterior inner wall, and the posterior outer wall with different asymmetry parameter at peak systolic pressure condition | 97 |

| | | |
|------|---|-----|
| 4.32 | Comparison between the Laplace Equation, Z.LI Equation the FSI solution and the linear fitting of the FSI solution with different asymmetry parameter | 98 |
| 4.33 | The velocity vectors at different stage of the second cardiac cycle through the three models at different wall thickness ($t = 0.05, 0.1, \text{ and } 0.2 \text{ cm}$) | 100 |
| 4.34 | The distributions of the Displacement Magnitude with different wall thickness at peak systolic pressure condition | 101 |
| 4.35 | The distributions of the Von Mises stress with different wall thickness at peak systolic pressure condition | 101 |
| 4.36 | Comparison between the Laplace Equation, Z.LI Equation the FSI solution and the linear fitting of the FSI solution with different wall thickness | 102 |
| 4.37 | The velocity vectors at different stage of the second cardiac cycle through the patient one at HBP, and NBP cases | 105 |
| 4.38 | The pressure distribution along the line in the patient's one wall, at different stage of the second cardiac cycle for HBP, and NBP cases | 106 |
| 4.39 | The velocity vectors at 1.3s and 1.4s through the two patients for HBP and NBP cases | 107 |
| 4.40 | The pressure distribution along the line in the two patient's wall at 1.3s and 1.4s for HBP, and NBP cases | 107 |
| 4.41 | The Displacement Magnitude distributions at different stage of the second cardiac cycle through the patient one for HBP, and NBP cases | 108 |
| 4.42 | The Von Mises stress distributions at different stage of the second cardiac cycle through the patient one for HBP, and NBP cases | 109 |
| 4.43 | The maximum Displacement Magnitude at different stage of the second cardiac cycle at the patient one for HBP, and NBP cases | 109 |
| 4.44 | The maximum Von Mises stress at different stage of the second cardiac cycle at the patient one for HBP, and NBP cases | 110 |
| 4.45 | The Von Mises stress distributions at 1.3s and 1.4s through the two patients for HBP, and NBP cases | 111 |

LIST OF SYMBOLS

| | | |
|-----------------|---|--|
| AAA | - | The Abdominal Aortic Aneurysm |
| CFD | - | The Computational Fluid Dynamic |
| CSS | - | The Computational Solid Stress |
| FSI | - | The Fluid-Structure Interaction analyses |
| CT | - | The Computed Tomography |
| MRI | - | The Magnetic Resonance Imaging |
| $f-FSI$ | - | The Fully coupling FSI |
| σ | - | The wall stress |
| P_i | - | The intra luminal Pressure |
| r | - | The vessel radius |
| t | - | The thickness of the wall vessel |
| ILT | - | The Intra luminal Thrombus |
| α | - | The Intra luminal Thrombus ratio |
| $A_{AAA,max}$ | - | The transverse areas of the AAA |
| $A_{ILT,max}$ | - | The Intra luminal Thrombus at the maximum AAA diameter location |
| $A_{Lumen,max}$ | - | The lumen area |
| $d_{AAA,max}$ | - | The aneurysm maximum diameter of AAA |
| H | - | The in-plane axis normal to the maximum diameter |
| $d_{Lumen,max}$ | - | The lumen diameter at the maximum AAA diameter location |
| L_{an} | - | The aneurysm length |
| L_{distal} | - | The distal length |
| ϕ | - | The bifurcation angle |
| β | - | The anterior posterior asymmetry parameter |
| I_p | - | The distances from the center of the end of the proximal to the posterior wall |

| | | |
|---------------------------|---|--|
| l_a | - | The distances from the center of the end of the proximal to the anterior wall |
| $r(z)$ | - | The diameter of each cross section |
| $\Delta_x(z)$ | - | The deviation of its centroid from the z-axis in x direction |
| $r_{prox,neck}$ | - | The Proximal neck radius |
| $L_{prox,neck}$ | - | The Proximal neck length |
| L_{AAA} | - | The aneurysm region length |
| $r_{distal,neck}$ | - | The distal neck radius |
| r_{iliac} | - | The iliac bifurcation radius |
| L_{iliac} | - | The iliac bifurcation length |
| L_{AA} | - | The interest region length |
| ρ_f | - | The constant fluid density |
| u_i | - | The velocity vector |
| c_j | - | The advective |
| \hat{u}_j | - | The velocity vector of the reference frame (mesh) |
| f_i^f | - | The body force at time t per unit mass, which is considered negligible as an AAA patient lies on a hospital during CT diagnosis. |
| τ_{ij}^f | - | The components of Cauchy stress tensor, which expressed as the combination of an isotropic pressure, and the stress tensor. |
| P | - | The isotropic pressure |
| δ_{ij} | - | The Kronecker delta |
| D | - | The rate of deformation tensor defined |
| $\dot{\gamma}_{ij}$ | - | The shear rate |
| $\eta(\dot{\gamma}_{ij})$ | - | The shear-dependent viscosity |
| ρ_s | - | The constant material density |
| d_i | - | The displacement vector |
| f_i^s | - | The body force at time t per unit mass, which is considered negligible as mention in fluid domain |
| τ_{ij}^s | - | The components of Cauchy stress tensor |
| W | - | The strain energy density. |
| W_D | - | The deviatoric strain energy density |
| W_V | - | The volumetric strain energy density |
| C_1, C_2 | - | The material constants |

| | | |
|----------------------------------|---|--|
| I_1 | - | The principal invariant of the Cauchy Green deformation tensor |
| C_{kkk} | - | The Cauchy Green deformation tensor |
| ϵ_{kkk} | - | The Green Lagrange strain tensor |
| δ_{kkk} | - | The Kronecker delta |
| J_3 | - | The reduced invariant |
| K | - | The bulk modulus |
| E | - | The Young's modulus |
| ν | - | The Poisson's ratio |
| \bar{P} | - | The weighting functions for the pressure |
| \bar{U} | - | The weighting functions for velocity |
| N | - | The total number of velocity nodes |
| K_p^T | - | The Divergence matrix |
| M | - | The Mass matrix |
| K_u | - | The Diffusion matrices |
| $N(c)$ | - | The Advection matrices |
| K_p | - | The Gradient matrices |
| R | - | The force vector describes the boundary condition |
| $\dot{d}_i^f n^f$ | - | The normal component of velocity in the FSI region of fluid domain |
| $u_{k\parallel}$ | - | The parallel component of the nodal velocity at the corresponding side or centre line. |
| $u_{k\perp}$ | - | The perpendicular component of the nodal velocity at the corresponding side or centre line |
| $H_{k\parallel}^u, H_{k\perp}^u$ | - | The interpolation functions for the parallel, and perpendicular component |
| Re_{ij}^e | - | The element Reynolds numbers on the side i - j |
| \hat{u}_{ij} | - | The average velocity on the side i - j |
| \bar{d}_i | - | The shape functions of displacement |
| ${}_0C_{ijrs}$ | - | The incremental stress strain tensors |
| ${}_0S_{ij}, {}_tS_{ij}$ | - | The second Piola Kirchoff stress tensor at time 0.0 referred to the configurations at time 0.0, and t respectively |
| ${}_0\epsilon_{ij}$ | - | The Green Lagrange strain tensor at time 0.0 referred to the configurations at time 0.0 |
| ${}_0e_{ij}$ | - | The linear incremental strains at time 0.0 referred to the configurations at time 0.0 |

| | | |
|----------------------|---|--|
| η_{ij} | - | The nonlinear incremental strains at time 0.0 referred to the configurations at time 0.0 |
| \bar{e}_{ij} | - | The linear incremental strains corresponding to the shape functions of displacement |
| $\bar{\eta}_{ij}$ | - | The nonlinear incremental strains corresponding to the shape functions of displacement |
| ${}^{t+\Delta t}f$ | - | The components of externally applied fluid force on the Γ_{FSI}^S |
| ${}^t_0K_L, {}^tK_L$ | - | The linear strain increment stiffness matrices |
| $B_L, {}^t_0B_L$ | - | The linear strain displacement transformation matrices |
| ${}_0C_0^t$ | - | The incremental stress strain material property matrices |
| ${}^t_0K_{NL}$ | - | The nonlinear strain (geometric or initial stress) incremental stiffness matrices |
| B_{NL} | - | The nonlinear strain displacement transformation matrices |
| t_0S | - | The matrix of the Second Piola Kirchhoff stress |
| H^S | - | The surface displacement interpolation matrices |
| t_0F | - | The vector of nodal point forces equivalent to the element stresses at time t |
| F_f, F_s | - | The linearized discrete equations of a fluid and solid equations |
| X_f, X_s | - | The fluid and solid vectors defined at fluid and solid nodes domains |
| λ_d | - | The displacement relaxation factor |
| λ_τ | - | The stress relaxation factor |
| R^2 | - | The coefficient of multiple determination |
| TSS | - | The total sum of square |
| SSE | - | The residual sum of squares |

LIST OF APPENDICES

| APPENDIX | TITLE | PAGE |
|-----------------|--------------|-------------|
| A | Publication | 133 |

CHAPTER 1

INTRODUCTION

1.1 Introduction

Abdominal aortic aneurysm (AAA) is an increase in the diameter of the aorta which is due to a weakness in the wall, that leads to rupture and it is considered as the 13th cause of death among both men and women in developed countries [1-4]. A surgical intervention can be done to avoid rupture, where the decision making is extensively based on the maximum aneurysm diameter ($D_{\max} > 5 \text{ cm}$ to 5.5 cm) and growth rate ($>1\text{cm/yr}$) [5-10]. Previous studies [11-19] have shown that the rupture would also occur in the small aneurysm (less than 5 cm), while in some special cases, which are considered big, it could reach to 10cm and there were no ruptures. It was concluded that the maximum aneurysm diameter criterion alone is not enough to predict the rupture, and other parameters for example smoking, family history, hypertension, intra luminal thrombus and geometry parameters (i.e. The aneurysm length, the maximum diameter, the length of distal neck, the iliac bifurcation angle, asymmetry and wall thickness) should also be taken into account to help the surgeons decide the need for surgical treatment to prevent delay, which can cause rupture, or early treatment, which is not without risk, especially for most patients older than seventy years old.

The rupture of aneurysm in biomechanical point of view is highly dependent on the ultimate stress and the acting stress on the wall, due to the effect of the hemodynamic. For this reason, recent researches have focused more on studying the mechanical properties of the aorta wall to find its ultimate strength and the stress acting upon it, and compared between them to predict the rupture. However, this work focuses on predicting the stress acting upon the wall, where there are many parameters that affect it, for example hypertension, intra luminal thrombus, and geometry parameters. These parameters can detect and measure very accurately by using ultrasound, computed tomography (CT scan) or magnetic resonance imaging (MRI).

Since there is no direct way to measure the acting stress on the AAA wall, the numerical methods; such as the Computational Fluid Dynamic (CFD), the Computational Solid Stress (CSS), and the Fluid-Structure Interaction (FSI), were widely used to compute it. Among these three methods, it has been proven that the FSI give the most accurate results because, it takes into account the effect of both hemodynamic and the wall structure. The different techniques of the FSI available for modeling the fluid and solid components are broken into three classifications, based on the level of coupling between fluid and solid, as shown in Figure 1.1.

The first classification is uncoupling, where the fluid equations are first solved to compute the pressure and velocity before passing the pressure at the interface as boundary condition to the solid analysis. The second classification is partial coupling, which is similar to the first one except that, also the displacements of the solid are used as boundary condition on the fluid domain at the end of time step without iteration. The third classification is known as fully coupling which can be divided into two methods (the partitioned method, and the direct method). The partitioned method is where the boundary data exchanges between the fluid and solid analysis for every time step and it is repeated until both systems have converged. The direct method, also known as Simultaneous solution method, is where the fluid equations and the solid equations are combined and treated in one system. The direct method has been used in this study because it is the fastest in the system of fully

coupled method and it is good for unsteady analysis.

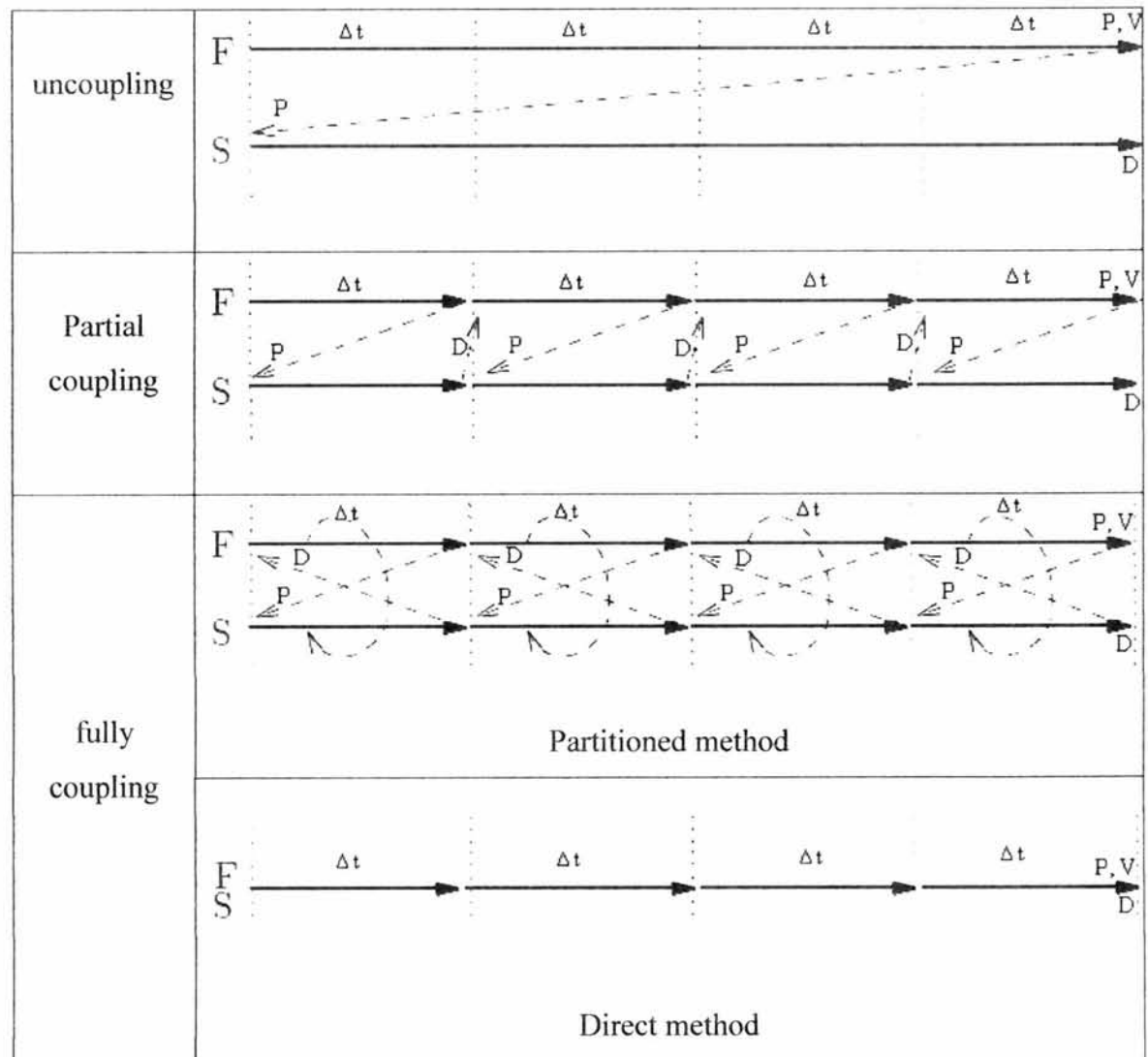


Figure 1.1 Fluid-Structure Interaction analyses producer [20].

On the other hand, it is important to mention here that the acting stress computed by the numerical method is considered as an expensive tool because it takes a long computational time and requires skilled staff to run the simulation. Therefore, it is helpful to come out with an equation that helps to save time and easy to use in calculating the maximum acting stress. Thereafter, it can be compared to the ultimate strength of the wall to predict the rupture of AAA.

1.2 Problem statement

Abdominal aortic aneurysm (AAA) is an increase in the diameter of the aorta that leads to its rupture. It is considered as the 13th cause of death in developed countries [1-4]. Numerous efforts have been done so far to prevent aneurysm rupture. Surgical intervention is one of the ways to prevent aneurysm rupture. It is considered necessary when the maximum aneurysm diameter is ($> 5-5.5$) cm, and growth rate ($> 1\text{yr/cm}$). Unfortunately, the surgeons who decide the need for surgical treatment rely on the rupture-predicting indicator (which is very often used alone). As a consequence, such an indicator cannot give an accurate reading when it is used alone. Instead, other parameters need be taken into account in order for to the surgeons to be able avoid the delay which can cause rupture, or early treatment which is not without risk especially most of the patients older than 70 years old.

Predicting the risk of the AAA rupture through determining the acting stress on its wall is a challenge that faces the researchers. Unfortunately, there is no direct method to measure it in the AAA. Although the numerical method has been widely used, yet, such a method requires both sufficient time and enough training. This in turn makes it too expensive method to be practically adopted. The correlation of some geometry parameters have also been studied [21-29], and semi empirical equation was developed by Z Li et al [28]. However, there are some limitations in this equation. It needs to be modified in order to get more accurate equation to predict the acting stress in AAA. Moreover, the Computational Solid Stress (CSS) analyses have been used to develop the Z Li equation. Unfortunately, they ignored the effect of the hemodynamic.

Unlike the previous attempts made by the researchers, this study takes into account the effect of both the hemodynamic and the deformation of the wall. This was conducted through using fully coupling-fluid structure interaction analysis (f-FSI) to modify the Z Li equation. In addition, the two new geometry parameters (the aneurysm length and the iliac bifurcation angle) have been added to it.

1.3 Objective of the Study

There are two main objectives in developing the new equation to predict the maximum acting wall stress for the purpose of estimating the risk of the Abdominal Aortic Aneurysm (AAA) rupture. They are:

- 1- To establish parametric correlations of some geometry parameters (the maximum aneurysm, the aneurysm length, the length of distal neck, the asymmetric parameter, the iliac bifurcation angle, and the wall thickness).

- 2- To develop the new equation to predict the maximum acting stress in AAA wall.

1.4 Scope of the Study

Several scopes have been recognized and found to be sufficient to develop the new equation to calculate the acting stress on the AAA wall to predict the risk of its rupture.

- i. The fully coupling fluid structure interaction analysis (f-FSI) has been used to create the dataset by simulate the virtual aneurysm models at different geometry parameters (the maximum aneurysm, the aneurysm length, the length of distal neck, the asymmetric parameter, the iliac bifurcation angle, and the wall thickness). MatLab code has been developed to generate the virtual aneurysm models.

- ii. The effect of these geometry parameters on the flow pattern, displacement and stress distributions have been studied by using the virtual aneurysm models.
- iii. The effect of the hypertension has been studied by used the real AAA models constructed from the CT scan.
- iv. The multiple linear regression method. and trial and error have been used to modified L Zi equation by using f-FSI dataset.
- v. The accuracy of the new equation was performed by comparing it to the equation currently used in the clinical indicator (Laplace equation), and Z Li equation, with numerical published datasets of the real AAA models, f-FSI simulation of the real AAA models driving from the CT scan, and f-FSI simulation of virtual aneurysm models in range out of that was used to developed the new model.

1.5 Outline of Thesis

This thesis is divided into the following chapters:

- 1- Introduction: Where the author has given a general overview of this work which includes the background of the work, some description of the f-FSI methods, the problem statement, objectives of the study and the scope of the study.

- 2- Literature review: Where the author has focused on the review of some previous studies that use the numerical method (CFD, CSS, FSI) to compute the wall stress, and other researchers that compare between these methods and also review of some articles that study the effect of some parameters in the wall stress and the strength of the AAA wall.
- 3- Methodology: The author has described in details the physiological variables that are used to study the influence in the maximum wall stress. In addition, the detailed descriptions on the construction of AAA geometry from the CT scan. The fluid and solid formulations as applicable to this application and the numerical procedure of the fluid structure interaction are introduced in Section 3.3. In the last section in this chapter, the procedure to develop the new model are described in details.
- 4- Result and Discussion: Where the validation of this f-FSI simulation is presented, and the effect of the Newtonian and Non-Newtonian properties on the wall shear stress distribution, the flow is shown and discussed in details, and also the effect of some geometry parameters (the maximum aneurysm, the aneurysm length, the length of distal neck, the asymmetric parameter, the iliac bifurcation angle, and the wall thickness), and hypertension, that have been discussed in this study. In the last section, the new model has been validated by comparing with the previous numerical study and also the fully coupling-fluid structure interaction (f-FSI) analysis by using modified models and the real models that have been constricted from the CT scan.
- 5- Conclusion: Where the conclusions and recommendations according to the objectives of the study are outlined. The suggestions for future work according to the limitation of this work are also highlighted.

REFERENCES

1. M. Law, Screening for Abdominal Aortic Aneurysms, *British Medical Bulletin*, 54. 1998. 903-913.
2. C. Fleming, E.P. Whitlock, T.L. Beil, F.A. Lederle, Screening for Abdominal Aortic Aneurysm: A Best-Evidence Systematic Review for the U.S. Preventive Services Task Force, *Annals of Internal Medicine*, 142. 2005. 203-211.
3. F.A. Lederle, R.L. Kane, R. MacDonald, Timothy J. Wilt, Systematic Review: Repair of Unruptured Abdominal Aortic Aneurysm, *Annals of Internal Medicine*, 146. 2007. 735-741.
4. R. Gillum, Epidemiology of Aortic Aneurysm in the United States, *Journal of Clinical Epidemiology*, 48. 1995. 1289-1298.
5. R.W. Thompson, P.J. Geraghty, J.K. Lee, Abdominal Aortic Aneurysms: Basic Mechanisms and Clinical Implications, *Current Problems in Surgery*, 39. 2002. 110-230.
6. D.A. Vorp, J.P.V. Geest, Biomechanical Determinants of Abdominal Aortic Aneurysm Rupture, *Journal of the American Heart Association*, 25. 2005. 1558-1566.
7. D.A. Vorp, Biomechanics of Abdominal Aortic Aneurysm, *Journal of Biomechanics*, 40. 2007. 1887-1902.
8. R. Limet, N. Sakalihassan, A. Albert, Determination of the Expansion Rate and Incidence of Rupture of Abdominal Aortic Aneurysms, *Journal of Vascular Surgery*, 14. 1991. 540-548.
9. C.B. Washington, J. Shum, S.C. Muluk, E.A. Finol, The Association of Wall Mechanics and Morphology: A Case Study of Abdominal Aortic Aneurysm Growth, *Journal of Biomechanical Engineering*, 133. 2011. 1-6.
10. A. Abbas, R. Attia, A. Smith, M. Waltham, Can We Predict Abdominal Aortic Aneurysm (AAA) Progression and Rupture by Non-Invasive Imaging?—A

- Systematic Review, *International Journal of Clinical Medicine*, 2. 2011. 484-499.
11. T.M. McGloughlin, B.J. Doyle, New Approaches to Abdominal Aortic Aneurysm Rupture Risk Assessment : Engineering Insights With Clinical Gain, *Journal of the American Heart Association*, 30. 2010. 1687-1694.
 12. J. Powell, L. Brown, J. Forbes, F. Fowkes, R. Greenhalgh, C. Ruckley, S. Thompson, Final 12-Year Follow-up of Surgery Versus Surveillance in the UK Small Aneurysm Trial, *British Journal of Surgery*, 94. 2007. 702-708.
 13. Z.-Y. Li, U. Sadat, J. U-King-Im, T.Y. Tang, D.J. Bowden, P.D. Hayes, J.H. Gillard, Association Between Aneurysm Shoulder Stress and Abdominal Aortic Aneurysm Expansion : A Longitudinal Follow-Up Study, *Journal of The American Heart Association*, 122. 2010. 1815-1822.
 14. R.J. Valentine, J.D. Decaprio, J.M. Castillo, J.G. Modrall, M.R. Jackson, G.P. Clagett, Watchful Waiting in Cases of Small Abdominal Aortic Aneurysms- Appropriate for all Patients, *Journal of Vascular Surgery*, 22. 2000. 441-450.
 15. F.A. Lederle, G.R. Johnson, S.E. Wilson, D.J. Ballard, W.D. Jordan, J. Blebea, F.N. Littooy, J.A. Freischlag, D. Bandyk, J.H. Rapp, A.A. Salam, Rupture Rate of Large Abdominal Aortic Aneurysms in Patients Refusing or Unfit for Elective Repair *Journal of the American Medical Association*, 287. 2002. 2968-2972.
 16. J.T. Powell, S.M. Gotensparre, M.J. Sweeting, L.C. Brown, F.G.R. Fowkes, S.G. Thompson, Rupture Rates of Small Abdominal Aortic Aneurysms: A Systematic Review of the Literature, *European Society for Vascular Surgery*, 41. 2010. 2-10.
 17. B.S. Cho, D.T. Woodrum, K.J. Roelofs, J.C. Stanley, P.K. Henke, G.R. Upchurch Jr, Differential Regulation of Aortic Growth in Male and Female Rodents Is Associated with AAA Development, *Journal of Surgical Research*, 2008. 1-9.
 18. L.W. van Laake, T. Vainas, R. Dammers, P.J.E.H.M. Kitslaar, A.P.G. Hoeks, G.W.H. Schurink, Systemic Dilation Diathesis in Patients with Abdominal Aortic Aneurysms: A Role for Matrix Metalloproteinase-9?, *European Journal of Vascular and Endovascular Surgery*, 29. 2005. 371-377.
 19. B. Louise C, P. Janat T, Risk Factors for Aneurysm Rupture in Patients Kept Under Ultrasound Surveillance, *Annals of Surgery*, 230. 1999. 289-297.

20. C.G. Giannopapa, Fluid Structure Interaction in Flexible Vessels, in, The University of London King's College London, London, 2004. 208.
21. D.A.Vorp, D.H.J.Wang, M.W.Webster, W.J.Federspiel, Effect of Intraluminal Thrombus Thickness and Bulbe Diameter on the Oxygen Diffusion in Abdominal Aortic Aneurysm, *Journal of Biomechanical Engineering*, 120. 1998. 579-583.
22. Z. Li, C. Kleinstreuer, A Comparison Between Different Asymmetric Abdominal Aortic Aneurysm Morphologies Employing Computational Fluid-Structure Interaction Analysis, *European Journal of Mechanics - B/Fluids*, 26. 2007. 615-631.
23. M.L. Raghavan, D.A. Vorp, Toward a biomechanical tool to evaluate rupture potential of abdominal aortic aneurysm: identification of a finite strain constitutive model and evaluation of its applicability, *Journal of Biomechanics*, 33. 2000. 475-482.
24. M. Xenos, Y. Alemu, D. Zamfir, S. Einav, J.J. Ricotta, N. Labropoulos, A. Tassiopoulos, D. Bluestein, The Effect of Angulation in Abdominal Aortic Aneurysms Fluid-Structure Interaction Simulations of Idealized Geometries, *Medical and Biological Engineering and Computing*, 48. 2010. 1175-1190.
25. E. Georgakarakos, C.V. Ioannou, Y. Kamarianakis, Y. Papaharilaou, T. Kostas, E. Manousaki, A.N. Katsamouris, The Role of Geometric Parameters in the Prediction of Abdominal Aortic Aneurysm Wall Stress, *European Journal of Vascular and Endovascular Surgery*, 39. 2010. 42-48.
26. B.J. Doyle, A. Callanan, P.E. Burke, P.A. Grace, M.T. Walsh, D.A. Vorp, T.M. McGloughlin, Vessel Asymmetry as an Additional Diagnostic Tool in the Assessment of Abdominal Aortic Aneurysms, *Journal of Vascular Surgery*, 49. 2009. 446-454.
27. L. Speelman, A. Bohra, E.M.H. Bosboom, G.W.H. Schurink, F.N. van de Vosse, M.S. Makaroun, D.A. Vorp, Effects of Wall Calcifications in Patient-Specific Wall Stress Analyses of Abdominal Aortic Aneurysms, *Journal of Biomechanical Engineering*, 129. 2007. 105-109.
28. Z. Li, C. Kleonstreuer, A New Wall Stress Equation for Aneurysm-Rupture Prediction, *Annals of Biomedical Engineering*, 33. 2005. 209-213.

29. C. Kleinstreuer, Z. Li, Analysis and Computer Program for Rupture-Risk Prediction of Abdominal Aortic Aneurysms, *BioMedical Engineering Online*, 5. 2006. 1-13.
30. H. Silaghi, A. Branchereau, S. Malikov, A. Andercou, Management of Small Asymptomatic Abdominal Aortic Aneurysms – A review, *International Journal of Angiology*, 4. 2007. 121-127.
31. J. Golledge, J. Abrokwah, K.N. Shenoy, R.H. Armour, Morphology of Ruptured Abdominal Aortic Aneurysms, *European Journal of Vascular and Endovascular Surgery*, 18. 1999. 96-104.
32. D. RC, M. CR, B. DC, O. LW, Autopsy Study of Unoperated Abdominal Aortic Aneurysms, *Circulation*, 56. 1977. 161–164.
33. J.P.V. Geest, D.H.J. Wang, S.R. Wisniewsk, M.S. Makaroun, D.A. Vorp, Towards A Noninvasive Method for Determination of Patient-Specific Wall Strength Distribution in Abdominal Aortic Aneurysms, *Annals of Biomedical Engineering*, 34. 2006. 1098-1106.
34. E.S.D. Martino, A. Bohra, J. P, V. Geest, N. Gupta, M.S. Makaroun, D. A, Biomechanical Properties of Ruptured Versus Electively Repaired Abdominal Aortic Aneurysm Wall Tissue, *Journal of Vascular Surgery*, 43. 2006. 571-576.
35. B.J. Wang, Makaroun, D.A. Webster, Effect of Intra luminal Thrombus on Local Abdominal Aortic Aneurysm Wall Strength, in: *BMESEMBS Conference*, 1999. 1.
36. E. Choke, G. Cockerill, W.R.W. Wilson, S. Sayed, J. Dawson, I. Loftus, M.M. Thompson, A Review of Biological Factors Implicated in Abdominal Aortic Aneurysm Rupture, *European Journal of Vascular and Endovascular Surgery*, 30. 2005. 227-244.
37. D.A. Vorp, M.L. Raghavan, M.W. Webster, Mechanical Wall Stress in Abdominal Aortic Aneurysm: Influence of Diameter and Asymmetry, *Journal of Vascular Surgery*, 27. 1998. 632-639.
38. A.K. Venkatasubramaniam, M.J. Fagan, T. Mehta, K.J. Mylankal, B. Ray, G. Kuhan, I.C. Chetter, P.T. McCollum, A Comparative Study of Aortic Wall Stress Using Finite Element Analysis for Ruptured and Non-ruptured Abdominal Aortic Aneurysms, *European Journal of Vascular and Endovascular Surgery*, 28. 2004. 168-176.

39. E.A. Finol, C.H. Amon, Flow-Induced Wall Shear Stress in Abdominal Aortic Aneurysms: Part I – Steady Flow Hemodynamics, *Computer Methods in Biomechanics and Biomedical Engineering*, 5. 2002. 309–318.
40. E.A. Finol, C.H. Amon, Flow-Induced Wall Shear Stress in Abdominal Aortic Aneurysms: Part II – Pulsatile Flow Hemodynamics, *Computer Methods in Biomechanics and Biomedical Engineering*, 5. 2002. 319–328.
41. Y. Papaharilaou, J.A. Ekaterinaris, The Influence of Asymmetric Inflow in Abdominal Aortic Aneurysm Hemodynamics, in: *European Conference on Computational Fluid Dynamics*, 2006. 1-9.
42. E. Boutsianis, M. Guala, U. Olgac, S. Wildermuth, K. Hoyer, Y. Ventikos, D. Poulidakos, CFD and PTV Steady Flow Investigation in an Anatomically Accurate Abdominal Aortic Aneurysm, *Journal of Biomechanical Engineering*, 131. 2009. 1-15.
43. K.M. Khanafer, J.L. Bull, J.G.R. Upchurch, R. Berguer, Turbulence Significantly Increases Pressure and Fluid Shear Stress in an Aortic Aneurysm Model under Resting and Exercise Flow Conditions, *Annals of Vascular Surgery*, 21. 2007. 67-74.
44. F.J.H. Gijsen, F.N. van de Vosse, J.D. Janssen, The Influence of the Non-Newtonian Properties of Blood on the Flow in Large Arteries: Steady Flow in a Carotid Bifurcation Model, *Journal of Biomechanics*, 32. 1999. 601-608.
45. F.J.H. Gijsen, E. Allanic, F.N. van de Vosse, J.D. Janssen, The Influence of the Non-Newtonian Properties of Blood on the Flow in Large Arteries: Unsteady Flow in a 90° Curved Tube, *Journal of Biomechanics*, 32. 1999. 705-713.
46. P. Rissland, Y. Alemu, S. Einav, J. Ricotta, D. Bluestein, Abdominal Aortic Aneurysm Risk of Rupture: Patient-Specific FSI Simulations Using Anisotropic Model, *Journal of Biomechanical Engineering*, 131. 2009. 1-10.
47. B.J.B.M. Wolters, M.C.M. Rutten, G.W.H. Schurink, U. Kose, J. de Hart, F.N. van de Vosse, A Patient-Specific Computational Model of Fluid-Structure Interaction in Abdominal Aortic Aneurysms, *Medical Engineering and Physics*, 27. 2005. 871-883.
48. T. Frauenfelder, M. Lotfey, T. Boehm, S. Wildermuth, Computational Fluid Dynamics: Hemodynamic Changes in Abdominal Aortic Aneurysm After Stent-Graft Implantation, *CardioVascular and Interventional Radiology*, 29. 2006. 613-623.

49. T.E. Tezduyar, M. Schwaab, S. Sathe, Sequentially-Coupled Arterial Fluid-Structure Interaction (SCAFSI) technique, *Computer Methods in Applied Mechanics and Engineering*, 1. 2008. 1-10.
50. Y. Papaharilaou, J.A. Ekaterinaris, E. Manousaki, A.N. Katsamouris, Stress Analysis in Abdominal Aortic Aneurysms Applying Flow Induced Wall Pressure, *GRACM International Congress on Computational Mechanics*, 5. 2005. 1-8.
51. J. Vimmr, A. Jonášová, Computer Simulation of Non-Newtonian Effects on Blood Flow in a Complete 3D Bypass Model in: 8th. World Congress on Computational Mechanics (WCCM8), 5th. European Congress on Computational Methods in Applied Sciences and Engineering (ECCOMAS 2008), 2008. 1-2.
52. K.M. Khanafer, P. Gadhoke, R. Berguer, J.L. Bull, Modeling Pulsatile Flow in Aortic Aneurysms: Effect of Non-Newtonian Properties of Blood, *Biorheology*, 43. 2006. 661-679.
53. E.A. Finol, E.S.D. Martino, D.A. Vorp, C.H. Amon, Fluid-Structure Interaction and Structural Analyses of an Aneurysm Model 2003 Summer Bioengineering Conference, 2003. 75.
54. C.M. Scotti, J. Jimenez, S.C. Muluk, E.A. Finol, Wall Stress and Flow Dynamics in Abdominal Aortic Aneurysms: Finite Element Analysis vs. Fluid-Structure Interaction, *Computer Methods in Biomechanics and Biomedical Engineering*, 11. 2008. 301-322.
55. C.M. Scotti, A.D. Shkolnik, S.C. Muluk, E.A. Finol, Fluid-Structure Interaction in Abdominal Aortic Aneurysms: Effects of Asymmetry and Wall Thickness, *BioMedical Engineering OnLine*, 4. 2005. 1-22.
56. C.M. Scotti, E.A. Finol, Compliant Biomechanics of Abdominal Aortic Aneurysms: a Fluid-Structure Interaction Study, *Computers & Structures*, 85. 2007 1097-1113.
57. J.-W. Hinnen, O.H.J. Koning, M.J.T. Visser, H.J. Van Bockel, Effect of Intraluminal Thrombus on Pressure Transmission in the Abdominal Aortic Aneurysm, *Journal of Vascular Surgery*, 42. 2005. 1176-1182.
58. G.W.H. Schurink, J.M.v. Baalen, M.J.T. Visser, J.H.v. Bockel, Thrombus within an Aortic not Reduce Pressure on the Aneurysm does Aneurysmal Wall, *Journal of Vascular Surgery*, 31. 2000. 501-506.

59. S.S. Hans, O. Jareunpoon, M. Balasubramaniam, G.B. Zelenock, Size and Location of Thrombus in Intact and Ruptured Abdominal Aortic Aneurysms, *Journal of Vascular Surgery*, 41. 2005. 584-588.
60. D.A. Vorp, P.C. Lee, D.H.J. Wang, M.S. Makaroun, E.M. Nemoto, S. Ogawa, M.W. Webster, Association of Intra luminal Thrombus in Abdominal Aortic Aneurysm with Local Hypoxia and Wall Weakening, *Journal of Vascular Surgery*, 34. 2001. 291-299.
61. J. H.Ashton, J.P.V. Geest, B. R.Simon, D.H. d, Compressive Mechanical Properties of the Intra luminal Thrombus in Abdominal Aortic Aneurysms and Fibrin-Based Thrombus Mimics, *Journal of Biomechanics*, 42. 2009. 197-201.
62. N. Sun, J. Leung, A. Wright, N. Cheshire, A. Hughes, S. Thom, Y. Xu, Modelling of Oxygen Transport in an Abdominal Aortic Aneurysm with Intra luminal Thrombus, *Journal of Biomechanics*, 41. 2008. 280-280.
63. W.R. Mower, W.J. Quiñones, S.S. Gambhir, Effect of Intraluminal Thrombus on Abdominal Aortic Aneurysm Wall Stress, *Journal of Vascular Surgery*, 26. 1997. 602-608.
64. E.S.D. Martino, D.A. Vorp, Effect of Variation in Intraluminal Thrombus Constitutive Properties on Abdominal Aortic Aneurysm Wall Stress, *Annals of Biomedical Engineering*, 31. 2003. 804-809.
65. M. Truijers, J.A. Pol, L.J. SchultzeKool, S.M. van Sterkenburg, M.F. Fillinger, J.D. Blankensteijn, Wall Stress Analysis in Small Asymptomatic, Symptomatic and Ruptured Abdominal Aortic Aneurysms, *European Journal of Vascular and Endovascular Surgery*, 33. 2007. 401-407.
66. K.M. Khanafer, J.L. Bull, R. Berguer, Fluid-Structure Interaction of Turbulent Pulsatile Flow within a Flexible Wall Axisymmetric Aortic Aneurysm Model, *European Journal of Mechanics - B/Fluids*, 28. 2009. 88-102.
67. T.W. Taylor, T. Yamaguchi, Three-Dimensional Simulation of Blood Flow in an Abdominal Aortic Aneurysm—Steady and Unsteady Flow Cases, *Journal of Biomechanical Engineering*, 116. 1994. 88-97.
68. D. Lee, J.Y. Chen, Pulsatile Flow Fields in a Model of Abdominal Aorta with its Peripheral Branches, *Biomedical Engineering Applications, Basis & Communications*, 15. 2003. 170-178.
69. J.H. Leung, A.R. Wright, N. Cheshire, J. Crane, S.A. Thom, A.D. Hughes, Y. Xu, Fluid Structure Interaction of Patient Specific Abdominal Aortic

- Aneurysms: a Comparison with Solid Stress Models BioMedical Engineering OnLine, 5. 2006. 1-15.
70. A. Sequeira, J. Janela, An Overview of Some Mathematical Models of Blood Rheology, in: A Portrait of State-of-the-Art Research at the Technical University of Lisbon, 2007. 65-87.
 71. L. JS, L. PC, C. SH., Turbulence Characteristics Downstream of Bileaflet Aortic Valve Prostheses, Journal of Biomechanical Engineering, 2. 2000. 118-124.
 72. E.A. Finol, K. Keyhani, C.H. Amon, The Effect of Asymmetry in Abdominal Aortic Aneurysms Under Physiologically Realistic Pulsatile Flow Conditions, Journal of Biomechanical Engineering, 125. 2003. 207-217.
 73. R. Adolph, D. Vorp, D.S. DL, M. Webster, M. Kameneva, S. Watkins, Cellular Content and Permeability of Intra luminal Thrombus in Abdominal Aortic Aneurysm, Journal of Vascular Surgery, 25. 1997. 916-926.
 74. S.H. Rambhia, M. Xenos, D. Bluestein, Fluid Structure Interaction for Patient Specific Risk Assessment in Ruptured Abdominal Aortic Aneurysms, in: Bioengineering Conference, 2010. 1-2.
 75. K.H. Fraser, M.-X. Li, W.T. Lee, W.J. Easson, P.R. Hoskins, Fluid-Structure Interaction in Axially Symmetric Models of Abdominal Aortic Aneurysms, Part H: Journal of Engineering in Medicine, 223. 2008. 195-209.
 76. A. Amblard, H.W.-L. Berre, B. Bou-Saïd, M. Brunet, Analysis of Type I Endoleaks in a Stented Abdominal Aortic Aneurysm, Medical Engineering & Physics, 2008. 1-7.
 77. Z. Li, C. Kleinstreuer, Blood Flow and Structure Interactions in a Stented Abdominal Aortic Aneurysm Model, Medical Engineering & Physics, 27. 2005. 369-382.
 78. Z. Li, C. Kleinstreuer, Computational Analysis of Type II Endoleaks in a Stented Abdominal Aortic Aneurysm Model, Journal of Biomechanics, 39. 2006. 2573-2582.
 79. M. L.Raghavan, B. Ma, R.E. Harbaugh, Quantified Aneurysm Shape and Rupture Risk, Journal of Neurosurgery, 102. 2005. 355-362.
 80. M. Bonert, R.L. Leask, J. Butany, C.R. Ethier, J.G. Myers, K.W. Johnston, M. Ojha, The Relationship Between Wall Shear Stress Distributions and Intimal Thickening in the Human Abdominal Aorta, BioMedical Engineering Online, 2. 2003. 1-14.

81. Y. Papaharilaou, J.A. Ekaterinaris, E. Manousaki, A.N. Katsamouris, A Decoupled Fluid Structure Approach for Estimating Wall Stress in Abdominal Aortic Aneurysms, *Journal of Biomechanics*, 40. 2007. 367-377.
82. A. Borghia, N.B. Wooda, R.H. Mohiaddinb, X.Y. Xua, Fluid–Solid Interaction Simulation of Flow and Stress Pattern in ThoracoAbdominal Aneurysms: A Patient-Specific Study, *Journal of Fluids and Structures*, 24. 2008. 270-280.
83. M.S. Sacks, D.A. Vorp, M.L. Raghavan, M.P. Federle, M.W. Webster, In Vivo Three-Dimensional Surface Geometry of Abdominal Aortic Aneurysms, *Annals of Biomedical Engineering*, 27. 1999. 469-479.
84. G. Giannoglou, G. Giannakoulas, J. Soulis, Y. Chatzizisis, T. Perdikides, N. Melas, G. Parcharidis, G. Louridas, Predicting the Risk of Rupture of Abdominal Aortic Aneurysms by Utilizing Various Geometrical Parameters: Revisiting the Diameter Criterion, *Angiology*, 57. 2006. 487-494.
85. J.F. Rodríguez, C. Ruiz, M. Doblaré, G.A. Holzapfel, Mechanical Stresses in Abdominal Aortic Aneurysms: Influence of Diameter, Asymmetry, and Material Anisotropy, *Journal of Biomechanical Engineering*, 130. 2008. 1-10.
86. Y. S.C.M, Steady and Pulsatile Flow Studies in Abdominal Aortic Aneurysm Models Using Particle Image Velocimetry, *International Journal of Heat and Fluid Flow*, 21. 2000. 74-83.
87. P. RA, R. TJ, B. EI., Pulsatile Flow in Fusiform Models of Abdoiminal Aortic Aneurysms: Flow Fields, Velocity Patterns and Flow-Induced Wall Stresses, *Jornal of Biomechanical Engineering*, 4. 2004. 438-446.
88. V. Deplano, Y. Knapp, E. Bertrand, E. Gaillard, Flow Behaviour in an Asymmetric Compliant Experimental Model for Abdominal Aortic Aneurysm, *Journal of Biomechanics*, 40. 2007. 2406-2413.
89. S. I.Bernad, E. S.Bernad, T. Barbat, R. Susan-Resiga, V. Albulescu, Effects of Asymmetry in Patient-Specific Wall Shear Stress Analyses of Abdominal Aortic Aneurysm, *Journal of Chinese Clinical Medicine*, 4. 2009. 1-14.
90. B.J. Doyle, T.J. Corbett, A. Callanan, M.T. Walsh, D.A. Vorp, T.M. McGloughlin, An Experimental and Numerical Comparison of the Rupture Locations of an Abdominal Aortic Aneurysm, *journal Endovasc Therapy*, 3, 2009. 322-335.
91. A.K. Venkatasubramaniam, M.J. Fagan, T. Mehta, K.J. Mylankal, B. Ray, G. Kuhan, I.C. Chetter, P.T. McCollum, A Comparative Study of Aortic Wall

- Stress Using Finite Element Analysis for Ruptured and Non-ruptured Abdominal Aortic Aneurysms, *Eur J Vasc Endovasc Surg*, 28. 2004. 168-176.
92. T. Hatakeyama, H. Shigematsu, T. Muto, Risk Factors for Rupture of Abdominal Aortic Aneurysm Based on Three-Dimensional Study, *Journal of Vascular Surgery*, 33. 2001. 453-461.
 93. F.L. Moll, J.T. Powell, G. Fraedrich, F. Verzini, S. Haulon, M. Waltham, J.A.v. Herwaarden, P.J.E. Holt, J.W.v. Keulen, B. Rantner, F.J.V. Schloßer, F. Setacci, J.-B. Ricco, Management of Abdominal Aortic Aneurysms Clinical Practice Guidelines of the European Society for Vascular Surgery, *European Journal of Vascular and Endovascular Surgery*, 41. 2011. S1-S58.
 94. D.R. Wong, W.C. Willett, E.B. Rimm, Smoking, Hypertension, Alcohol Consumption, and Risk of Abdominal Aortic Aneurysm in Men, *American Journal of Epidemiology*, 165. 2007. 838-845.
 95. J.F. Blanchard, H.K. Armenian, P.P. Friesen, Risk Factors for Abdominal Aortic Aneurysm: Results of a Case-Control Study, *American Journal of Epidemiology*, 151. 2000. 575-583.
 96. K. Singh, K.H. Bønaa, B.K. Jacobsen, L. Bjørk, S. Solberg, Prevalence of and Risk Factors for Abdominal Aortic Aneurysms in a Population-based Study, *American Journal of Epidemiology*, 154. 2001. 236-244.
 97. L. Morris, P. O'Donnell, P. Delassus, T.M. Gloughlin, Experimental Assessment of Stress Patterns in Abdominal Aortic Aneurysms Using the Photoelastic Method *An International Journal for Experimental Mechanics*, 40. 2004. 165-172.
 98. B.J. Doyle, A. Callanan, T.M. McGloughlin, A comparison of Modelling Techniques for Computing Wall Stress in Abdominal Aortic Aneurysms, *Biomechanical Engineering Online*, 6. 2007. 1-12.
 99. J.F. Rodríguez, C. Ruiz, G. Holzapfel, M. Doblaré, Mechanical Stress in Abdominal Aneurysm: Influence of Geometry and Material Anisotropy, *Journal of Biomechanics*, 39. 2006. S272-S273.
 100. M. Fillinger, M. Raghavan, S. Marra, J. Cronenwett, F. Kennedy, In Vivo Analysis of Mechanical Wall Stress and Abdominal Aortic Aneurysm Rupture Risk, *Journal of Vascular Surgery*, 36. 2002. 589-597.

- Stress Using Finite Element Analysis for Ruptured and Non-ruptured Abdominal Aortic Aneurysms, *Eur J Vasc Endovasc Surg*, 28. 2004. 168-176.
92. T. Hatakeyama, H. Shigematsu, T. Muto, Risk Factors for Rupture of Abdominal Aortic Aneurysm Based on Three-Dimensional Study, *Journal of Vascular Surgery*, 33. 2001. 453-461.
 93. F.L. Moll, J.T. Powell, G. Fraedrich, F. Verzini, S. Haulon, M. Waltham, J.A.v. Herwaarden, P.J.E. Holt, J.W.v. Keulen, B. Rantner, F.J.V. Schlo"sser, F. Setacci, J.-B. Ricco, Management of Abdominal Aortic Aneurysms Clinical Practice Guidelines of the European Society for Vascular Surgery, *European Journal of Vascular and Endovascular Surgery*, 41. 2011. S1-S58.
 94. D.R. Wong, W.C. Willett, E.B. Rimm, Smoking, Hypertension, Alcohol Consumption, and Risk of Abdominal Aortic Aneurysm in Men, *American Journal of Epidemiology*, 165. 2007. 838-845.
 95. J.F. Blanchard, H.K. Armenian, P.P. Friesen, Risk Factors for Abdominal Aortic Aneurysm: Results of a Case-Control Study, *American Journal of Epidemiology*, 151. 2000. 575-583.
 96. K. Singh, K.H. Bønaa, B.K. Jacobsen, L. Bjørk, S. Solberg, Prevalence of and Risk Factors for Abdominal Aortic Aneurysms in a Population-based Study, *American Journal of Epidemiology*, 154. 2001. 236-244.
 97. L. Morris, P. O'Donnell, P. Delassus, T.M. Gloughlin, Experimental Assessment of Stress Patterns in Abdominal Aortic Aneurysms Using the Photoelastic Method *An International Journal for Experimental Mechanics*, 40. 2004. 165-172.
 98. B.J. Doyle, A. Callanan, T.M. McGloughlin, A comparison of Modelling Techniques for Computing Wall Stress in Abdominal Aortic Aneurysms, *Biomechanical Engineering Online*, 6. 2007. 1-12.
 99. J.F. Rodríguez, C. Ruiz, G. Holzapfel, M. Doblaré, Mechanical Stress in Abdominal Aneurysm: Influence of Geometry and Material Anisotropy, *Journal of Biomechanics*, 39. 2006. S272-S273.
 100. M. Fillinger, M. Raghavan, S. Marra, J. Cronenwett, F. Kennedy, In Vivo Analysis of Mechanical Wall Stress and Abdominal Aortic Aneurysm Rupture Risk, *Journal of Vascular Surgery*, 36. 2002. 589-597.

101. M. Fillinger, S. Marra, M. Raghavan, F. Kennedy, Prediction of Rupture Risk in Abdominal Aortic Aneurysm During Observation: Wall Stress Versus Diameter, *Journal of Vascular Surgery*, 37. 2003. 724-732.
102. M.L. Raghavan, D.A. Vorp, M.P. Federle, M.S. Makaroun, M.W. Webster, Wall Stress Distribution on Three Dimensionally Reconstructed Models of Human Abdominal Aortic Aneurysm, *Journal of Vascular Surgery*, 31. 2000. 760-769.
103. M.L. Raghavan, M.W. Webster, D.A. Vorp, Ex Vivo Biomechanical Behavior of Abdominal Aortic Aneurysm: Assessment Using a New Mathematical Model *Annals of Biomedical Engineering*, 24. 1996. 573-582.
104. C. Taylor, T. Hughes, C. Zarins, Finite Element Modeling of Three-Dimensional Pulsatile Flow in the Abdominal Aorta: Relevance to Atherosclerosis, *Annals of Biomedical Engineering*, 26. 1998. 975-987.